Synthesis and characterization of a phosphorous/nitrogen based sol-gel coating as a novel halogen- and formaldehyde-free flame retardant finishing for cotton fabric

Accepted Manuscript

Synthesis and characterization of a phosphorous/nitrogen based sol-gel coating as a novel halogen- and formaldehyde-free flame retardant finishing for cotton fabric

Angela Castellano, Claudio Colleoni, Giuseppina Iacono, Alessio Mezzi, Maria Rosaria Plutino, Giulio Malucelli, Giuseppe Rosace

PII: S0141-3910(19)30057-6

DOI: https://doi.org/10.1016/j.polymdegradstab.2019.02.006

Reference: PDST 8782

To appear in: *Polymer Degradation and Stability*

Received Date: 21 November 2018

Revised Date: 25 January 2019

Accepted Date: 4 February 2019

Please cite this article as: Castellano A, Colleoni C, Iacono G, Mezzi A, Plutino MR, Malucelli G, Rosace G, Synthesis and characterization of a phosphorous/nitrogen based sol-gel coating as a novel halogen- and formaldehyde-free flame retardant finishing for cotton fabric, *Polymer Degradation and Stability* (2019), doi: https://doi.org/10.1016/j.polymdegradstab.2019.02.006.

Synthesis and characterization of a phosphorous/nitrogen based sol-gel coating as a novel halogen- and formaldehyde- free flame retardant finishing for cotton fabric

Angela Castellano[1], Claudio Colleoni[1], Giuseppina Iacono[2], Alessio Mezzi[3], Maria Rosaria Plutino[4,*], Giulio Malucelli[2,*], Giuseppe Rosace[1,*]

[1] *Department of Engineering and Applied Sciences, University of Bergamo, Viale Marconi 5, 24044, Dalmine (BG) Italy*

[2] *Department of Applied Science and Technology, Politecnico di Torino, Viale T. Michel 5, 15121, Alessandria, Italy*

[3] *Institute for the Study of Nanostructured Materials, ISMN – CNR, via Salaria Km29.3, 00015 Monterotondo stazione (Rome), Italy.*

[4] *Institute for the Study of Nanostructured Materials, ISMN – CNR, O.U. Palermo, c/o Department of ChiBioFarAm, University of Messina, Viale F. Stagno d'Alcontres 31, Vill. S. Agata, 98166 Messina, Italy.*

Abstract

A novel formaldehyde- and halogen-free coating, containing phosphorus, nitrogen and silicon, was synthesized with a promising approach to enhance flame retardancy of cotton fabric. To this aim, a new sol-gel precursor, comprising in the same molecule P, N and Si, namely (3-Glycidyloxypropyl)triethoxysilane modified N-(phosphonomethyl) iminodiacetic acid (PGPTES), was co-hydrolysed and co-condensated with tetraethylorthosilicate (TEOS), as silane linker, and used for producing a self-extinguishing cotton fabric coating. The structure of PGPTES was characterized by $^{1}H/^{13}C/^{31}P$ nuclear magnetic resonance and the obtained coating was investigated by FT-Infrared Spectroscopy and Scanning Electron Microscopy. The thermal properties of the treated fabric were studied by Thermogravimetric Analyses and Cone Calorimetry Tests. The

obtained results show that the synthetized coating is able to catalyse the dehydration and char formation of cellulose based polymer at a lower temperature, thanks to the thermal decomposition of phosphate giving rise to acidic intermediates, able to further react with cellulose-based fabric, hence improving the flame retardant properties of the latter.

Keywords: Sol-gel; GPTES; N-(Phosphonomethyl)iminodiacetic acid; Textile finishing; flame retardancy.

1. Introduction

Recently, nanotechnology has become a fast-growing area of research in the textile field because of its many potential applications allowing the development and evolution of a new class of improved materials [1]. Advanced applications have been developing through textile or textile-based materials, such as nanofibers, as well as nanocomposite fibres [2]. Meanwhile, nanoparticles are also successfully being used in conventional textiles to impart new functionalities and improved performance [3, 4]. In fact, they have high surface energy and a large surface area-to-volume ratio, which makes them easy to be linked to the treated substrate, increasing the durability of the functions imparted to textile materials [5]. Currently, one of the biggest scientific and technological challenges is the design of new materials in order to develop innovative applications. In this context, the role of preparative chemistry is to provide the compounds useful for obtaining innovative materials: among them, hybrids exploit the peculiarities of both the organic and the inorganic chemistries, hence giving rise to an almost unlimited number of applications. As an alternative to chemistry employed for the surface modification, a range of solution techniques have emerged, including co-precipitation, hydrothermal processing, solvothermal methods and sol–gel chemistry [6]. Among these, the sol–gel approach shows some particular advantages, being centred on the ability to produce a solid-state material from a chemically homogeneous precursor. The "Design" of sol-gel materials - and their material properties - is to some extent possible by changing

the chemical composition and arrangement of the molecular building blocks and by deliberately tailoring their nano- and micro-structure. The sol-gel technique, consisting in hydrolysis and condensation reactions, is based on hydrolysable precursors-building blocks - mostly metal or semi-metal alkoxides (precursors); among them, the most widely studied are silicon alkoxides, characterized by the strong covalent Si-O bonding and a hydrophobic behaviour that makes them immiscible with polar media. In textile applications, the most representative precursors are organofunctional trialkoxysilanes (R'-Si$(OR)_3$), because of their unique structure bearing three polimerizable groups, which enables the formation of a highly oriented polymer network structure with an incorporated organic moiety.

The sol-gel process represents a simple method for the development of a coating with selected protective properties, presenting many advantages, such as the possibility to achieve an environmentally-friendly surface functionalization of substrates and the easy adaptation of this finishing process to the existing processing lines in industrial scale production [10–13]. Depending on the chemical structure of the network-modifying moiety, different functional properties can be tailored on the material surface. Among these, it is worthy to mention antimicrobial [14], UV radiation protection [15,16], biomolecule immobilization [17], dye fastness [16,18], anti-wrinkle finishing [19] and super-hydrophobicity [20], as well as antistatic properties, odour control, stimuli-responsive performance [21] and strength enhancements [22]. In addition, since silica coatings exert a thermal shielding effect on polymer surfaces improving the flame retardancy of the treated fabrics [23], the use of sol-gel methods for conferring flame retardant properties to textile fabrics, in particular cellulose-based fibres, has been documented by several research groups [24]. In fact, cotton, thanks to its peculiarities such as strength, durability, flexibility and air permeability, as well as good biocompatibility, low cost and good mechanical properties [25], is one of the most important materials employed not only for producing apparel but also home furnishings and industrial products, namely medical supplies, industrial thread and tarpaulins [26]. Unfortunately, this cellulosic material has a low limiting oxygen index (LOI) and combustion temperature that

makes it highly flammable [27]. In order to meet fire safety regulations and expand the use of cotton in textile applications that require flame resistance, a significant number of flame retardant treatments has been developed in the last century [28], among which formaldehyde-based and halogenated compounds have been the most employed. Although they show high performance with excellent washing fastness, in most of them, the presence of active hydroxymethyl units causes the release of formaldehyde from the treated fabrics both during the fabric application and throughout the lifetime of the garment, which is not environmentally compatible [29]. For what concerns halogenated compounds, recently, research studies regarding their persistence, ability to bio-accumulate, and potential for toxicity have led to increasing restrictions and regulations on the production and use of some of them. In particular, such compounds as polybrominated biphenyls, penta and octobromodiphenilethers have been banned, as they could generate corrosive and toxic combustion products (e.g. dioxins and furans). [30]. Given the negative impact of formaldehyde and bromine-based finishes on human health, since they are carcinogenic and bio-accumulative, respectively, it is a primary focus for public safety to develop equivalent compounds, without formaldehyde and halogens. Replacing the above-mentioned flame retardants finishes with environmentally-friendly compounds represents an ecological step forward, in agreement with IPPC European Directive [31]. Phosphorus-based flame retardants seem to be a valid alternative for the above-mentioned FRs: in fact, unlike the halogen-containing compounds, which generate toxic gases, corrosive smoke, or harmful substances [30], they act in condensed phase, by converting into phosphoric acid or metaphosphoric acid during combustion or thermal degradation. Thus, non-volatile polyphosphoric acids can react with the decomposing polymer by esterification and dehydration to promote the formation of protective char [32]. The development of the latter provide lower flammability to fabric by protecting the underlying polymer from attack by oxygen and radiant heat. Besides, it was found that organophosphorus containing active nitrogen have multifunctional advantages and show higher effectiveness if compared with pure phosphorus counterparts: a) low toxicity during combustion, b) high efficiency measured by cone calorimeter,

and c) low smoke development in fire accidents [6]. Some nitrogen-containing compounds seem to accelerate phosphorylation of cellulose through the formation of a phosphorus-nitrogen polymeric species, and thus synergize the flame retardant action of phosphorus. The reason could be attributed to the type of bond between elements: P-N bonds are more polar than the already present P-O bonds, and the enhanced electrophilicity of the phosphorus atom increases its ability to phosphorylate the C(6) primary hydroxyl group of cellulose. By this way, the intra- molecular C(6)-C(1) rearrangement reaction forming levoglucosan is blocked. Meanwhile, the auto-crosslinking of cellulose promotes and consolidates the char formation derived by the action of the same flame retardants [33,34]. In addition to the above-mentioned compounds, silicon is demonstrated to be used as a flame-retardant element because it is able to produce a continuous layer of silica that retards char oxidation.

In this paper, we take advantage of the synergistic effect between silica and phosphorous in conferring flame retardant properties: in fact, the concurrent presence of P and Si elements in the same precursor can be exploited for preparing a hybrid coating that behave, at the same time, as a char promoter (with the same above-mentioned mechanism) and thermal shield, due to the metal-oxide ceramic network [35–40].

In this study, (3-Glycidyloxypropyl)triethoxysilane (GPTES), one of the most used silica precursors for hybrid silica-based textile finishing, was chosen since its ethoxysilyl groups and the reactive epoxy group allow promoting the adhesion with the treated textile surface and the reaction with other organic molecules, respectively. Furthermore, the epoxy ring can be simultaneously crosslinked, via extended covalent bonds, to form poly- or oligo-(ethylene oxide) derivatives, thus allowing the grow-up of a hybrid polyoxyethylene 3D-network. Carboxylic moieties of N-(phosphonomethyl) iminodiacetic acid (PMIDA), a nitrogen-containing carboxyphosphonate, react with GPTES epoxy groups to form a β-hydroxy propyl ester, following the mechanism proposed in Fig 1.

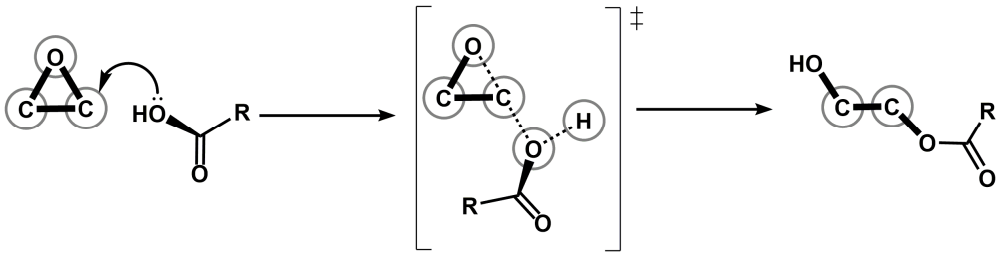

Fig. 1. Proposed mechanism of reaction between PMIDA and GPTES.

Combining the advantages of a facile synthesis with the use of a traditional application procedure, the proposed phosphorus-functionalized sol-gel precursor (PGPTES) emerges as promising candidate for next-generation of hybrid finishes based on the concurrent presence of Si, P and N, with breakthrough performances. Considering that PGPTES possesses both an inorganic moiety and a high phosphorus content, it is potential for serving as a facile~~, eco-friendly~~ and efficient flame retardant agent for cellulosic fibres. Furthermore, the mild reaction conditions of the process make it very favourable for the deposition of a hybrid organic-inorganic coating during the finishing of cotton fabrics. In this research, the structure and surface morphology of the untreated and treated cotton fabric were investigated in detail by NMR and FT-IR spectroscopy and Scanning Electron Microscopy (SEM), equipped with an energy dispersive X-ray spectroscopy (EDX). Then, the surface chemical composition was investigated by X-ray Photoelectron Spectroscopy (XPS). Thermogravimetric analysis (TGA), cone calorimetry (CC), horizontal and vertical flame spread tests were exploited for evaluating the combustion behaviour, the thermal stability, as well as the flammability of the treated cotton samples.

2 Experimental part

2.1. Materials

(3-Glycidyloxypropyl)triethoxysilane (GPTES, namely: $Si(OC_2H_5)_3C_3H_5O_2$), ≥98%)) and

Tetraethoxysilane (TEOS, namely: $Si(OC_2H_5)_4$), ≥98%) as sol–gel precursors, as well as N-(Phosphonomethyl)iminodiacetic acid hydrate (PMIDA, 97%, MW 227.11), monoethanolamine (MEA), and HCl (all reagent grades) were purchased from Sigma Aldrich (Italy) and used without any further purification. Scoured and bleached plain-weave cotton fabrics, with an areal density of 237 g/m^2, were supplied by Mascioni Spa, Varese, Italy. In order to remove impurities that would scatter on the fabric surface randomly during manufacturing, before sol-gel treatments, all the fabrics were carefully cleaned by washing in a 2% non-ionic detergent (Tergipal NRZ, linear alcohol ethoxylate, kindly supplied by FTR SpA, Italy) at 40 °C for 20 min, then rinsed several times with de-ionized water, and finally dried. Before all experiments, all the samples were placed under standard laboratory conditions 65(±4) % relative humidity and 20(±2) °C temperature) for 24 h.

2.2 Nanosol preparation and application process

Pre-reacted precursor sol was initially prepared from a mixture of high purity GPTES and PMIDA. To promote the reaction between the epoxy group and the hydroxyl groups of the phosphonate, the reaction was carried out in the absence of water, with the goal of limiting the possibility that the epoxy group can either undergo hydrolysis to form the corresponding diol or polyaddition reactions and polyether linkages. Therefore, 10 g of PMIDA powder, finely grinded, were slowly added to 20 ml of a TEOS/GPTES mixture (precursors molar ratio 25:75) into a 100 ml flask. The mixture was kept for 2 h at room temperature, under vigorous stirring, until the solution became clear. Finally, in order to start stepwise hydrolysis and condensation of oligomeric intermediate, 18.5 ml of water were added. Monoethanolamine (MEA) was used for adjusting the pH to 3 and to increase the nitrogen content of the FR system. The so-obtained solution was stirred for 3 h to complete the hydrolysis of both precursors. With the aim to produce the xerogel and investigate its chemical

178 structure, small amounts of the obtained sol were applied on glass slides, the solvent was removed
179 at 80°C for 1 h and the thin film was then cured at 170°C for 1 h.
180 The cotton fabrics (20 cm x 30 cm) were dipped in the hybrid sol and then passed through a two-
181 roll laboratory padding machine at nip pressure of 3 bar with about 75% of wet pick-up. After
182 drying at 90°C for 5 min, the fabric sample was cured at 170°C in a laboratory oven for 5 min. The
183 treated cotton sample was coded as CO_T. The amount of coating deposited, calculated as add-on
184 on the untreated sample (A, wt% owf), was calculated weighing the sample before (W_0) and after
185 the padding-curing treatment (W_1), using a Mettler balance (10^{-4} g):

186 $$A = \frac{W_1 - W_0}{W_0} \times 100 \qquad \text{Eq. 1}$$

187 The value obtained from Eq. 1 represents the average of five independent replicates, with the
188 standard deviation always lower than ±2%.
189
190 *2.3 Characterization*
191
192 FTIR spectra of treated and untreated cotton samples were recorded using a Thermo Avatar 370
193 spectrophotometer equipped with an attenuated total reflectance (ATR) device for solids analysis.
194 Spectra were analysed using Omnic 7.3 software. Fabrics were stored at room temperature for 48 h
195 in a stabilized atmosphere at 20°C and 60% RH. The analysis was performed with the samples
196 placed onto a diamond crystal, within 4000 and 650 cm^{-1}, with 64 scans and a resolution of 4 cm^{-1}.
197 The collected spectra were normalized to the 1314 cm^{-1} band, associated with the C-H bending
198 mode of cellulose. Since infrared absorption bands of the silica-based coating applied onto the
199 fabric surface are covered by the strong vibrational peaks of cellulose, FTIR analysis was carried
200 out also on pure xerogel in order to characterize it, thereby avoiding other influences. In addition,
201 based on the intensity and shift of vibrational bands of FTIR spectra, the treated sample was
202 compared with pristine cotton in order to assess the presence of the coating. The morphologies of

treated and untreated cotton fabrics, including the char residues after horizontal flame spread tests, were observed using scanning electron microscopy (LEO-1450VP, with beam voltage fixed at 5 kV), equipped with an X-ray probe (INCA Energy Oxford, Cu-Ka X- ray source, k_α= 1.540562 Å), which was utilized for performing elemental analysis. Thermogravimetric analyses (TGA) were carried out on a TAQ500 apparatus, using a heating rate of 20°C/min in nitrogen and air atmosphere (gas flow: 60 mL/min for both the atmospheres). The experimental error was ±0.5% on the weight and ±1°C on the temperature. Combustion tests of square fabric samples (50 mm x 50 mm x 0.5 mm) were carried out on a Fire Testing Technology Ltd Cone Calorimeter, under ventilated conditions, using a 35 kW/m^2 irradiative heat flow in horizontal configuration. The experiments were repeated four times for each material investigated to ensure reproducible and significant data; the experimental error was within 3%. The following parameters were registered: time to ignition (TTI, s), peak of heat release rate (pkHRR, kW/m^2), total heat release (THR, assessed at the end of the test, MJ/m^2), ratio of carbon dioxide and carbon monoxide yields, and final residue (%). The accuracy was up to 3 and 10% for CO and CO_2 yields, respectively. A Fire Performance Index (FPI, %/s) was also calculated as final residue to TTI ratio and employed as an evaluating parameter: the higher the FPI value, the better the flammability performance.

The flammability of the cotton samples in the presence of a flame spread was measured both in horizontal and vertical configurations.

In the first case, the flame was applied on the short side of the specimen (50 mm) for 10 s and then removed rapidly. Two horizontal marks were drawn on the specimens (at 25 and 75 mm from the side, on which the flame was applied) and the time (t_1 and t_2) required to the flame to reach them was measured. Besides, other relevant parameters, such as total burning time and final residue, were evaluated. Alternatively, when the test was performed in vertical configuration, a methane flame was applied for 5 s at the bottom of a fabric specimen (50 mm x 100 mm), repeating the test 3 times for each formulation in order to get reproducible data. A Flammability Performance Index (FPI, %/s) was also calculated as the ratio of final residue to the total burning time and used as an

evaluation parameter: the higher the FPI values, the better is the flame retardancy performance. Prior to flammability and combustion tests, all the specimens were conditioned at 23±1 °C for 48 h at 50% R.H. in a climatic chamber.

^{1}H, $^{13}C\{^{1}H\}$ and $^{31}P\{^{1}H\}$ NMR spectra were recorded in D_2O solutions or in a CD_3OD/D_2O mixture (1:1=v/v) at 500, 125 and 202 MHz, respectively; coupling constants (*J*) are given in hertz, and the attributions are supported by heteronuclear single-quantum and multi-bond coherence (HSQC-HMBC) and correlation spectroscopy (COSY) experiments; all proton NMR experiments were run with a water suppression pulse sequence.

XPS measurements were performed by using a ESCALAB MkII spectrometer equipped with a non-monochromatized Al Kα source and a five channeltrons detection system. The samples were fixed to the holder by metallic clip. The spectra were collected at 40 eV pass energy and the binding energy scale was calibrated positioning the C 1s peak form adventitious carbon at BE = 285.0 eV. All data were collected and processed by Avantage v.5 software.

3. Results and Discussion

3.1 NMR characterization and structure determination

The PGPTES xerogel film, covering a glass-slide, was carefully removed, chopped and suspended in a CD_3OD/D_2O mixture (1:1=v/v), in order to characterize the silylated derivative by means of homonuclear and heteronuclear ^{1}H, $^{13}C\{^{1}H\}$ and $^{31}P\{^{1}H\}$ NMR, mono- and bidimensional NMR spectroscopy. Figure 2 shows the recorded $^{31}P\{^{1}H\}$, ^{1}H, and $^{13}C\{^{1}H\}$ NMR stacked plots, respectively, in comparison with the starting PMIDA molecule (on the bottom of the figures, in D_2O) and the suspended xerogel coating TEOS_GPTES_PMIDA (PGPTES), in a 1/1 CD_3OD/D_2O mixture.

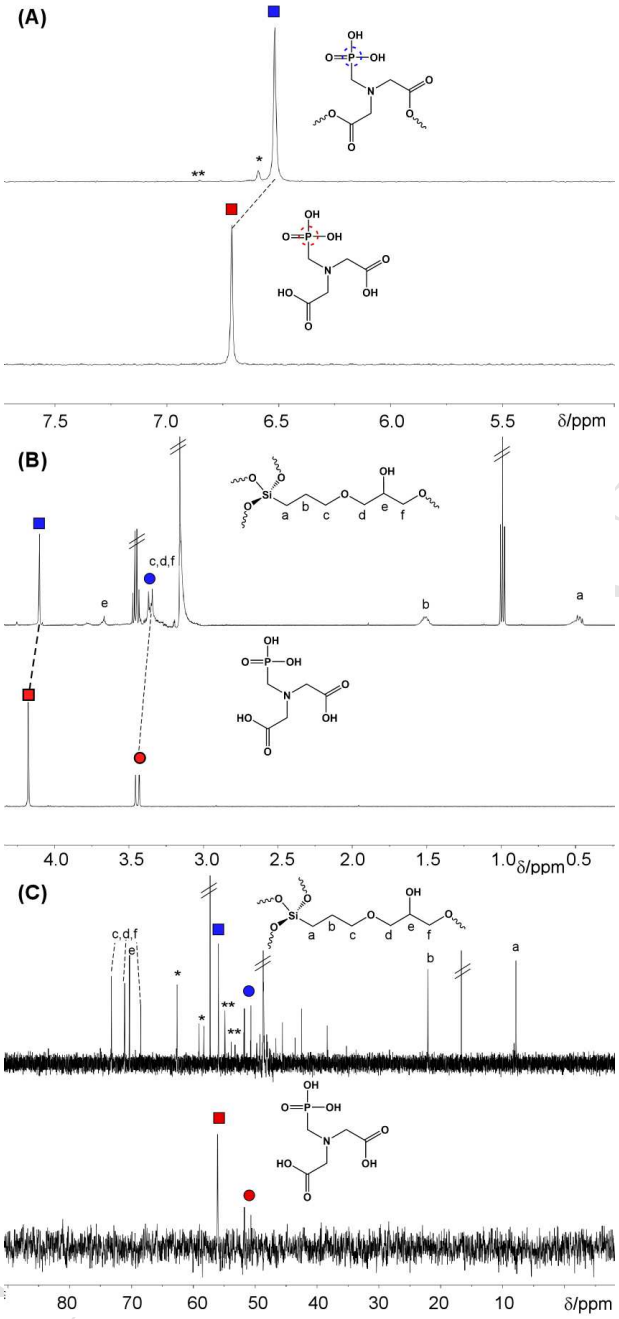

Fig. 2. Stacked NMR spectra relative to a solution of starting PMIDA molecule in D_2O (bottom) and a suspension of PGPTES xerogel (top) in a CD_3OD/D_2O (1:1=v/v) mixture as solvent at 298 K: **A.** $^{31}P\{^1H\}$ NMR (202 MHz); **B.** ^1H NMR, with the main proton assignment; (500 MHz); **C.** $^{13}C\{^1H\}$ NMR, with the main carbon assignment (125 MHz).

The $^{31}P\{^1H\}$ NMR spectra in Figure 2A clearly shows the expected lower frequency shift of the ^{31}P signal relative to the PMIDA molecule from δ = 6.71 (red square) to 6.52 ppm (blue square),

evidencing that a more shielding environment is enclosing the ^{31}P nucleus of the PMIDA~~,~~ after ~~the~~ reaction with GPTES. Two minor ^{31}P containing species are present in solution at very slight concentration (highlighted in Figure 2A with a star and double stars).

In agreement, the aliphatic regions of the ^{1}H NMR spectra in figure 2B clearly show: (i) the corresponding upfield proton shifts for the two methylene groups CH_2-COOH and CH_2-P, that shift from δ = 4.17 and 3.44 (m, $^{2}J_{PH}$=12.3Hz) ppm, to δ = 4.10 and 3.36 (m, $^{1}J_{PH}$=12.5Hz) ppm, respectively (red square and circle *vs* blue square and circle); (ii) the presence of the expected protonic pattern for the GPTES open ring derivative, bringing a hydroxyl and an ester group bonded to two vicinal carbon C_e and C_f atoms (δ = 0.47, CH_{2a}; 1.51, CH_{2b}; 3.36, CH_{2c}+CH_{2d}+CH_{2f}; 3.66 CH_{2e}), in a 2:1 concentration ratio with respect to protons belonging to the PMIDA molecule [41–43]; (iii) the presence of the methylene and the methyl proton resonances relative to free ethanol moieties.

Similar results can be drawn with the assignments of the ^{13}C{^{1}H} NMR spectra, shown in figure 2C, that undoubtedly display: (i) the presence of the pattern expected for the PMIDA_GPTES fragments, characterized by almost the same ^{13}C chemical shift for the carboxylic group and for the two methylene CH_2-*C*OOH and CH_2-P, as well as the starting PMIDA molecule (i.e. δ = 168.6; 55.9, $^{3}J_{PC}$ = 3.4 Hz; 51.3 ppm, $^{1}J_{PC}$=136 Hz *vs* δ = 168.4; 56.1, $^{3}J_{PC}$ = 2.6 Hz; 51.2 ppm, $^{1}J_{PC}$=135 Hz, respectively); (ii) diol, dioxane and polyethyleneoxide silylated functionalities (not assigned peaks) embedded in the final xerogel matrix [43], together with other minor phosphorous containing PMIDA derivatives (star and double stars).

All these findings confirm that the GPTES epoxy ring opening reaction has successfully taken place, combined with the complete hydrolysis of the alkoxysilane end group. Even if solvent effects (due to a 50% CD_3OD presence as solvent for the PGPTES spectra) should be taken into account especially in the ^{1}H spectra assignments, the high and already well-known nucleophilic substitution reactivity of the carboxylic groups towards the epoxy rings [42,44] led us to conclude that, in the final xerogel, the PMIDA molecule is mainly bonded firmly and covalently through two ester bonds

to the sol-gel based 3D matrix [45,46]; minor species may be assigned most probably to the monosubstituted ester species or to the fully substituted species through the two acetic groups and the phosphorous end. As previously shown, the epoxy ring opening of GPTES gives rise to the formation of diol and silylated dioxane/polyether (PEO), through several hydrolysis and polymerization reaction steps [43].

According to the reported results, a scheme of the occurred reaction is presented in Fig. 3 showing the formation of a N-(Phosphonomethyl)imino diacetate hydroxy polysiloxane derivative through a starting 1:2 molecular species, namely N-(Phosphonomethyl)imino bis{2-hydroxy-3-[3-(triethoxysilane)propoxy]propyl acetate]}.

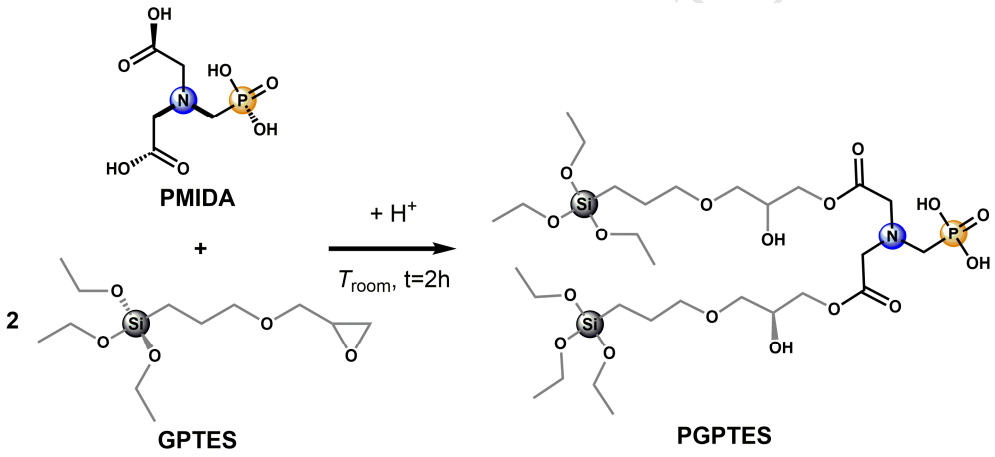

Fig. 3 Scheme of the reaction occurring between PMIDA and GPTES

3.2 SEM-EDX analysis

Scanning electron microscopy was utilized to investigate the morphological features of untreated and coated cotton fabrics. Fig. 4 shows SEM micrographs of cotton and the related EDX spectra before and after hybrid sol-treatment. The latter results in 25.2% add-on, calculated according to equation 1. In both magnifications, images of the untreated cotton sample show a flat assembly with a twisted ribbon-like structure caused by spiralling of cellulose fibrils. The surface appears clearly smooth with its veined natural morphology. After treatment, fibres are homogeneously covered by

the hybrid coating, showing free gaps between the warp and weft threads that maintain the same aspect of the control cotton fabric, suggesting that the sol-gel coating on the treated sample is very thin. Furthermore, semi-quantitative EDX investigation, employing a high beam voltage (i.e. 20 kV), confirms the key information concerning the element composition of samples. With the aim of assessing the homogeneous distribution of coatings, five repeated measurements were carried out on different parts of each cotton sample. Although the maps reported in the images are qualitative, in the treated samples only phosphorus and silicon are present, along with carbon and oxygen shown in the control fabric, since the technique cannot detect nitrogen atom. Furthermore, the data listed in Tab. 1 show very similar results in all repeated tests, confirming a uniform presence of the above-mentioned elements on the treated fabric sample.

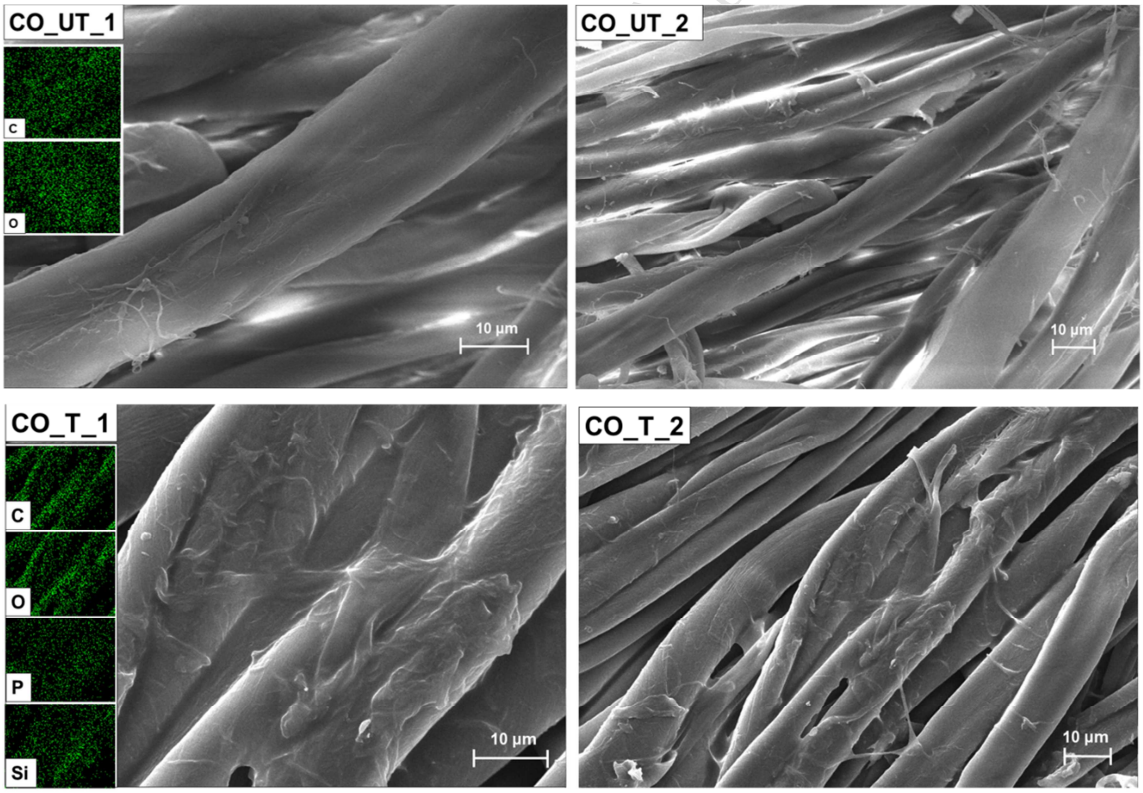

Fig. 4. SEM images of untreated (CO_UT) and treated (CO_T) cotton samples, at different magnifications, coded as _1, _2, for x2.50 K, x1.00 K, respectively.

Table 1.

Results (wt.%) of EDX analysis of untreated and treated samples.

Sample		C [%]	O [%]	P [%]	Si [%]
CO_UT	Unburned	46.10±0.07	53.9 ± 0.50	/	/
	Burned*	/	/	/	/
CO_T	Unburned	44.19±0.03	49.32±0.73	2.63±0.58	3.86±0.87
	Burned	60.53±1.33	30.01±0.54	5.9±1.51	4.23±0.06

* no residue was collected after flammability test.

3.3 XPS analysis

In order to investigate the surface chemical composition of both coated and untreated cotton fabrics, the samples were investigated by XPS analysis. The presence of C and O was registered on both samples, while the coated sample also showed the presence of Si, P and N. The shape of the C 1s signal (Fig. 5(a)) was characteristic for cotton fabric, characterized by three peaks positioned at BE = 285.0 eV, 286.7 eV and 288.5 eV, with intensity ratio 1 : 1.1 : 0.2, and assigned to C–C/C–H, C–OH and C=O bonds, respectively. The sol-gel coating slightly modified the shape of C 1s signal (Fig. 5(b)), because it was very thin. However, the formation of the sol-gel coating was confirmed by the presence of Si, P and N. After flammability tests, the shape of C 1s signal significantly changed (Fig. 5(c)), where the intensity ratio of the peaks became 1 : 0.3 : 0.1 and a fourth peak was positioned at BE = 291.4 eV, due to the presence of carbonates. This changing was not unexpected, because it is typically for residual char samples [47]. Comparing the XPS quantitative analysis, shown in Tab. 2, it can be noted that sol-gel coating was partially decomposed during the flammability test, with a decrease of the atomic concentration of Si and an accumulation of P and C

elements on the outermost layers of the substrate. These last results may appear inconsistent with those obtained by EDX analysis (Table 1). This is due to the different depth of each analysis. In fact, XPS technique investigates the first layer of the sample (< 10 nm), while information depth of EDX is approximately 1 μm. Furthermore, the results are comparable (e.g. Si/P ratio) even if they are given in wt% (EDX) and in at. % (XPS).

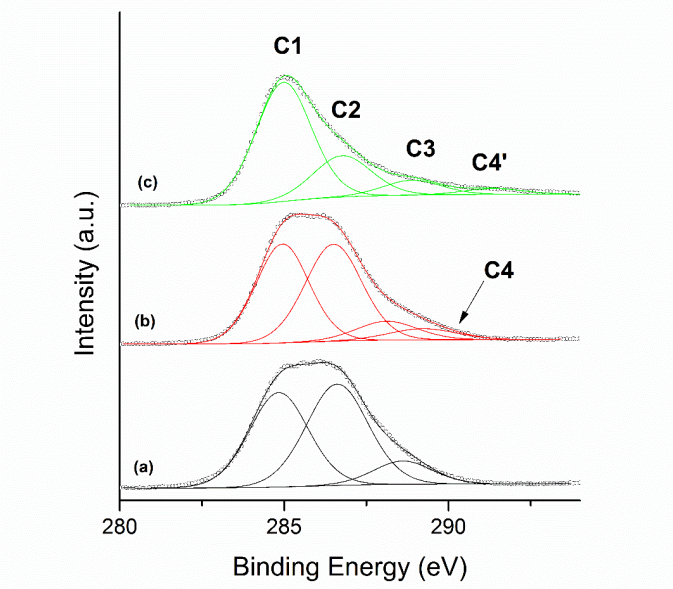

Fig. 5. Comparison of C 1s spectra of (a) untreated cotton fabric (CO_UT), (b) treated cotton fabric (CO_T) and (c) carbonaceous char (CO_C).

Table 2.

Surface chemical composition of the untreated cotton fabric (CO_UT), treated cotton fabric (CO_T) and carbonaceous char (CO_C).

	C (%)					N (%)	O (%)	P (%)	Si (%)
	C1: C-C/C-H	**C2: C-OH**	**C3: C=O**	**C4: - COOH**	**C4´: CO_3^-**	**NR_3**	**-OH**	**Phosphate**	**SiOR**
BE (eV)	285.0	286.6	288.1	289.2	291.4	400.5	532.8	133.7	103.3
CO_UT	29.1	32.7	7.2				31.0		
CO_T	26.4	27.6	5.8	3.7		2.3	29.1	1.7	3.5

CO_C	42.3	15.4	5.6	2.2	3.7	24.3	4.6	2.1

359

360 **3.4 ATR-FTIR spectroscopy**

361

362 The ATR-FTIR spectra of the untreated, treated cotton fabrics and pure xerogel prepared on glass
363 slides, are compared in Fig. 6 and the most important bands are collected in Table 3. The analytical
364 measurement of modified GPTES hybrid sol has been carried out, since the strong vibrational bands
365 of the pure substrate could hide the characteristic peaks of the thin film applied onto the fabric
366 surface. Comparing the xerogel spectrum with that of PMIDA, it can be highlighted the absence of
367 a broad band at 2650-2450 cm^{-1}, characteristic of such type of compounds and attributed to P-OH
368 stretching vibration. Also the band at 929 cm^{-1}, typical of P-OH bending signal, disappears. These
369 findings, combined with the shift of the stretching vibration of P=O from 1215 cm^{-1} to higher
370 wavenumbers (1267 cm^{-1}), demonstrate an effective interaction between phosphorous compound
371 and silica matrix. The other characteristic peaks that can be seen from xerogel spectrum are located
372 at 1736 cm^{-1} (stretching vibration of ester carbonyl), at 1635 cm^{-1} and 1540-1520 cm^{-1} (typical of
373 the absorption of NH_2 group). The region between 1200 and 750 cm^{-1} includes peaks characteristics
374 of silicon matrix: 1194 cm^{-1} (Si-O-Si asymmetric stretching), 1045 cm^{-1} (Si-O-Si), 1009 cm^{-1} (Si-O
375 stretching), 907-930 cm^{-1} (Si-OH stretching), 763-790 cm^{-1} (Si-O-Si symmetric stretching).
376 Moreover, the opening of the epoxide ring was observed through the absence of its characteristic
377 infrared bands at 1255 cm^{-1} (ring breathing), 907 cm^{-1} (asymmetric ring deformation) and 851
378 cm^{-1} (symmetric ring deformation) [46, 48]. FTIR spectroscopy was also carried out in order to
379 confirm the successful reaction between the hybrid coating and cotton. As shown in Figure 5, the
380 spectrum of untreated cotton exhibits O–H stretching absorption between 3500 and 3000 cm^{-1}, C–H
381 stretching absorption around 2950–2850 cm^{-1}, and C–O–C stretching absorption around 1160 cm^{-1}.
382 These bands are consistent with those of the typical cellulose backbone. The spectrum of the coated
383 cotton appears quite similar to that of the untreated one. With respect to the latter, an overall slight

384 decrease of the intensities of characteristic hydrogen-bonded OH stretching vibrations is observed:
385 this finding may be attributed to the interaction of the coating with the cotton functional groups. In
386 the treated cotton sample, some new characteristic peaks appear, such as the broad absorption band
387 in the region 2970-2850, which is attributed to the introduction of the $–CH_2$ group; these peaks are
388 proportional to the quantity of carbon included in the grafted molecules and, in particular, the band
389 of asymmetric stretching vibration of the methylene group located at 2925-2970 cm^{-1} and a band
390 attributable to symmetric stretching vibration at 2850- 2920 cm^{-1} can be detected. The absorption
391 band at 1732 cm^{-1} was assigned to the stretching vibration of carbonyl of ester group [49]. The
392 majority of the peaks typical of $-PO_3$ moiety are hidden by intense cellulose bands; the only one that
393 is clearly visible is at 1269 cm^{-1}, assigned to the P=O stretching vibration. The most important
394 peaks attributable to the sol-gel coating were identified at 1008, 930 and 765 cm^{-1} assigned to Si-O-
395 Si asymmetric stretching, Si-OH stretching, and Si-O-Si symmetric stretching, respectively. The
396 peak expected to be at about 1040 cm^{-1} is overlapped with a broad band between 1050 and 1014
397 cm^{-1} attributed to the characteristic peaks of cellulose. Some changing in the intensity of IR bands
398 appearing onto the treated textile fabric in the range between 1240 and 1160 cm^{-1} are assigned to
399 Si-O-C bonds, thus confirming the reaction between the hydrolysed silane precursor and the
400 cellulosic substrate. Although these peaks may be considered weak, they are of great importance
401 because they are a proof of the interaction between the substrate and the precursor [50].
402 Furthermore, the presence of amino group from MEA is observed at about 1629 and 1526 cm^{-1} due
403 to symmetric and asymmetric N-H bending modes, respectively.

404

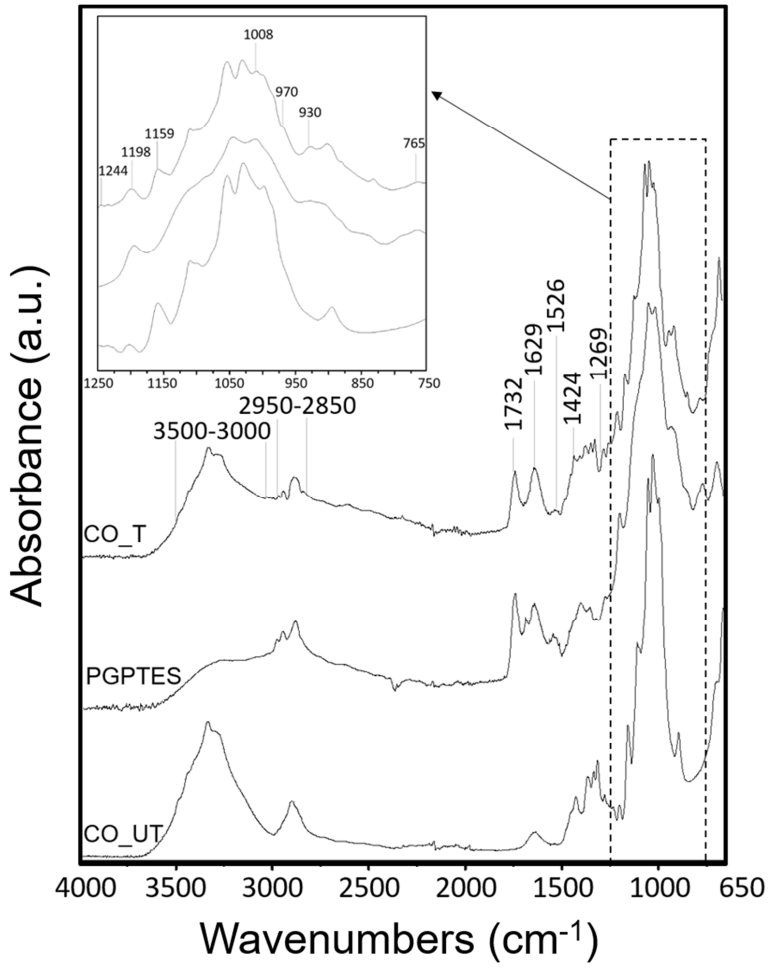

405

406 **Fig. 6.** AT-FT IR of hybrid coating onto glass slide (PGPTES), untreated (CO_UT) and treated

407 cotton (CO_T) samples.

408

409 **Table 3**

410 Major vibrational frequencies of the sol-gel based films.

Experimental wavenumbers (cm^{-1})		**Literature wavenumbers**	**Vibrational mode**
Glass substrate	**Fabric substrate**	**(cm^{-1})**	
3300	3500–3000	3500–3000 [51]	ν (O-H)
2850	2950–2850	2980–2800 [51]	ν (C-H)

1736	1732	1735 [52]	ν (C=O)
1635, 1540-1520	1629, 1526	1600, 1575 [53]	ν (N-H)
–	1424	1429 [51]	ω (C-H)
1266	1269	1267 [54]	ν P=O
–	1244	1240 [55]	Si-O-C
1194	1198	1200 [51]	ν_{as}(Si-O-Si)
–	1159	1160 [51]	ν_{as} C-O-C
1009	1008	1001 [51]	ν (Si-O-Si)
907-930	930	952 [51]	ν (Si-OH)
790-763	765	749–786 [51]	ν_s (Si-O-Si)

411

412 **3.5 Thermal behaviour**

413 The thermal and thermo-oxidative stability of the untreated and sol-gel treated cotton fabrics has
414 been assessed by thermogravimetric analyses performed in nitrogen and air, respectively.

415 The TG and dTG thermograms of sol-gel treated and untreated cotton samples are shown in Fig. 7;
416 Table 4 collects the corresponding data in terms of T_{onset}, T_{max} (corresponding to the peak(s) in dTG

curves) and related residues and final residue at 700°C. For both the environments, the weight loss up to 100°C, due to absorbed moisture in all samples, was not considered for this degradation study. In nitrogen, the TG curves of untreated cotton sample show the onset degradation temperature at about 310°C, together with its maximum mass loss rate at about 360°C, due to depolymerization by trans-glycosylation reactions. The coated fabric shows an anticipation in the onset degradation temperature, reaching the maximum mass loss rate at 275°C: this finding is attributed to the earlier degradation of the phosphorus-containing compound that catalyses the decomposition of cotton towards the formation of a carbonaceous residue (char). This latter increases the thermal stability of the fabric: in fact, at the end of the test, the char residue achieves 38%, significantly higher than pure cotton, for which the residue is below 6%.

In air, the thermo-oxidation of cotton takes place in a similar way: the only difference is for the appearance of a second degradation step at high temperatures (T_{max2}: 460°C). This phenomenon can be attributed to the oxidation of the char formed during the first step and of all the hydrocarbon species still present [56]. Once again, the hybrid coating is responsible for the decrease of both T_{onset} and T_{max1} as well as for the increase of the residues at T_{max1}, T_{max2} and 700°C: these findings confirm the protective effect exerted by the formed stable char.

Compared to untreated cotton control, the effectiveness of the silica-based coating as a flame retardant for cotton, directly attributable to the considerably higher energy and ionic character of the Si-O bond (443.7 kJ/mol) relative to the C-C bond (345.7 kJ/mol) [57], is indicated by a substantial lowering of the decomposition temperature, due to the earlier degradation of the phosphorus contained in the modified precursor, which is able to catalyse the dehydration of the treated cotton to form the intumescent char. As confirmed by TGA results, the higher the residue in the silica-phosphorylated cotton, the lower is the amount of volatile products obtained upon decomposition of the samples during the test.

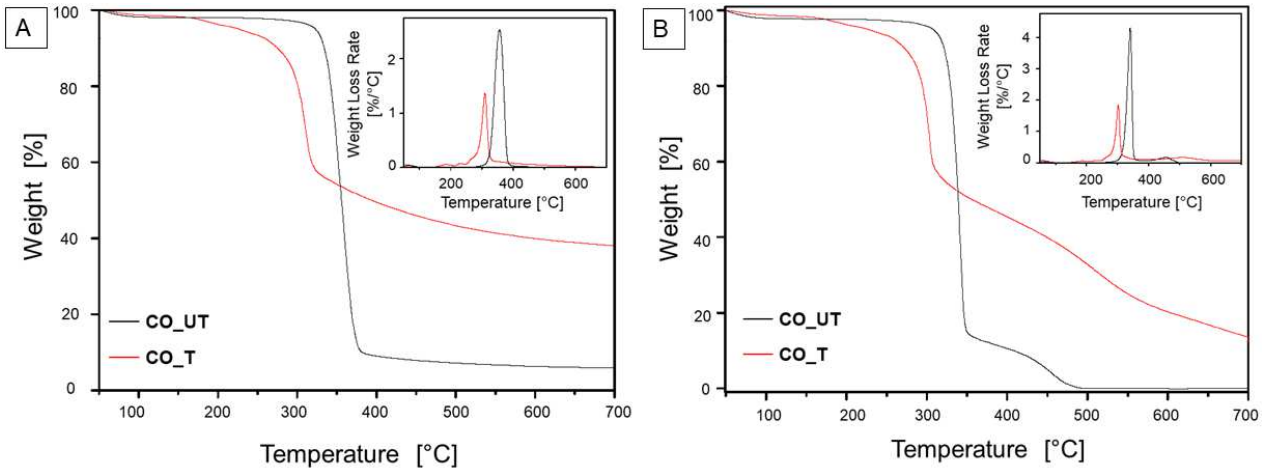

Fig. 7. TG and dTG curves of CO_UT and CO_T samples, in: **A.** nitrogen and **B.** air atmospheres.

Table 4.

Sample	T_{onset} (°C) (s)	T_{max1}* (°C)	Residue @T_{max1} (%)	T_{max2}* (°C)	Residue @T_{max2} (%)	Residue @700°C (%)
			Atmosphere: Nitrogen			
CO_UT	310	360	40	/	/	5.8
CO_T	275	310	70	/	/	38
			Atmosphere: Air			
CO_UT	300	340	46	460	3.2	/
CO_T	260	300	73	520	30	12

TG data for CO_UT and CO_T in nitrogen and air.

* from dTG curves

449 **3.6 Cone calorimetry tests**

450

451 The forced-combustion behaviour of cotton samples was investigated through cone calorimetry
452 tests, measuring the time to ignition (TTI), the peak heat release rate (pkHRR), the total heat release
453 (THR) and the final residue (%), as well as CO and CO_2 yields (%).
454 The curves of HRR vs. time for control and silica-coated fabric are shown in Fig. 8B. From Tab. 5,
455 it can be seen that if compared to untreated cotton, the coated fabric shows a reduction in both heat
456 release rate peak (pkHRR) and in the total heat release (THR). In fact, with respect to the uncoated
457 sample, in the treated fabric pkHRR decreases from 154 to 135 kW/m^2, corresponding to an
458 approximately 12% reduction. The THR also drops significantly, going from 3.9 down to 2.3
459 MJ/m^2. In the case of coated sample, it is worthy to note that after ignition, the HRR value increases
460 rapidly in a very short time (from 25 to 40 s) and then decreases sharply. This behaviour is
461 attributable to the formation of an intumescent char instantly after ignition by the phosphorus-
462 containing silica coating, indicating that more cotton fabric participates in the carbonization
463 process, due to the presence of the deposited coating. Consequently, less degradation products that
464 serve as “fuel” go into the gas phase, hence lowering the pkHRR and THR values. In addition, in
465 order to evaluate the fire performance index (FPI), the ratio between final residue and pkHRR
466 values for treated and untreated samples was calculated. The FPI value of the control cotton is
467 0.023 %/s, whereas that for silica coated cotton is 0.76 %/s. The higher FPI value for the coated
468 cotton sample justifies the higher amount of final residue and the shorter time to ignition with
469 respect to the untreated counterpart. Based upon the aforementioned fire behaviour, it is believed
470 that the formation of intumescent char layer is responsible for suppressing fire propagation at the
471 selected heat flux, or greatly inhibiting the amount of flammable gases available for combustion.
472 Finally, through CO and CO_2 analysis it is possible to provide useful information on the mechanism
473 of decomposition of cotton fabrics, since low CO_2/CO ratio means low conversion of CO to CO_2,
474 thus suggesting inefficiency of combustion. When cotton fabrics were treated with PGPTES, the

CO production changed a little, whereas the CO_2 production was decreased, leading to a remarkable decrease of CO_2/CO ratio (19.5). This suggests that the designed flame retardant mainly acts in condensed phase. It should be remarked that the char residues from cone calorimeter tests, reported in Figure 8A, are consistent with high-temperature residues obtained by TG analysis. The poor residue from the neat sample was completely broken, hence confirming the low charring ability of cellulose. On the other hand, the residue of the coated sample shows a coherent and dense char, maintaining a compact structure and its original texture. This is a direct consequence of the silica precursor formulation containing phosphorus and nitrogen. In fact, both species can synergistically act [28,51], catalysing the formation of the char layer that limits the heat and mass transfer, thus reducing the formation of flammable gases. At the same time, this char was made more stable by the beneficial presence of silica that does not allow the fire spread.

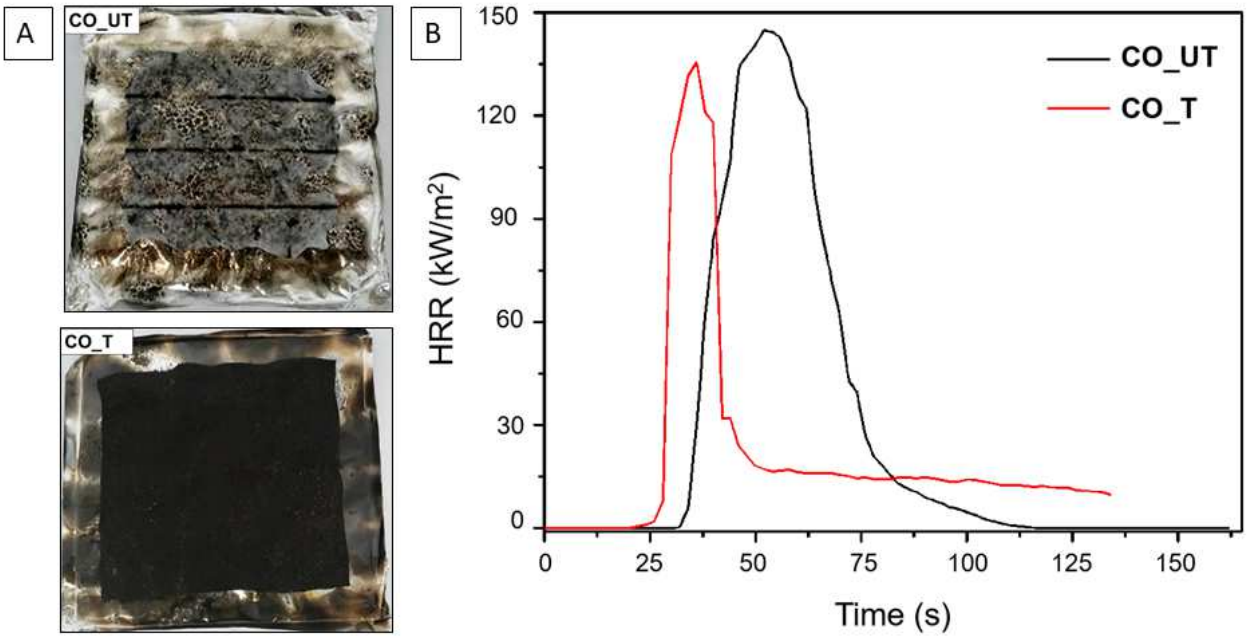

Fig. 8. **A.** Residues of CO_UT and CO_T from cone calorimetry tests performed at 35 kW/m^2; **B.** Heat release (HRR) curves of CO_UT and CO_T.

Table 5.

Combustion data of CO_UT and CO_T from cone calorimetry tests performed at 35 kW/m^2

Sample	TTI (s)	Flame out (s)	pkHRR (kW/m^2)	THR (MJ/m^2)	Residue (%)	CO (%)	CO_2 (%)	CO_2/CO
CO_UT	43±2	75	154±4	3.9±0.1	1	0.0014	0.20	143
CO_T	34±2	48	135±3	2.3±0.1	26	0.0087	0.17	20

3.7 Flammability tests

In order to evaluate flame retardant performance, the uncoated and coated fabrics were subjected to horizontal and vertical flame spread tests. The images of the burned samples, together with the flammability data (after flame time, afterglow time and residue (%)), for both vertical and horizontal configurations, are presented in Table 6. At the end of the tests, the residues the uncoated fabrics have been completely destroyed, leaving only few amounts of ash, whereas for the treated sample there was only smoulder progression of fire that stopped before the scribed line for measurement. More in detail, in horizontal configuration, immediately after ignition, on the untreated sample a vigorous flame appears for about 23 s, followed by 139 s of afterglow that did not leave any residue. Conversely, the treated fabric sample shows no visible after-flame time, and very short after-glow time (8 s) and achieves self-extinction a few seconds after the flame application. As a result, at the end of combustion, the residue is 99.5% and the Flammability Performance Index (FPI) is 12.44%/s. Also in vertical configuration, the untreated cotton fabric is fully consumed during the test; conversely, the treated sample completely stops the flame propagation almost as soon as the flame is removed, showing neither afterflame, nor afterglow and

obtaining self-extinguishing classification. Once again, the results confirm the good behaviour of the phosphorous and nitrogen containing sol-gel coating onto cotton fibres, as a dehydrating and char-forming layer, which hinders heat, fuel and oxygen transmission by creating a ceramic barrier onto the treated fabric surface from further burning.

Table 6

Flammability behaviour and data related to the horizontal and vertical tests of CO_UT and CO_T samples.

	Data	CO_UT	CO_T
Horizontal configuration	t_1 (s)	**23**	**8**
	t_2 (s)	**76**	**0**
	Total burning time (s)	**139**	**8**
	Residue (%)	**0**	**99.5**
	FPI (%/s)	**0**	**12.44**
	Self-extinction	NO	YES

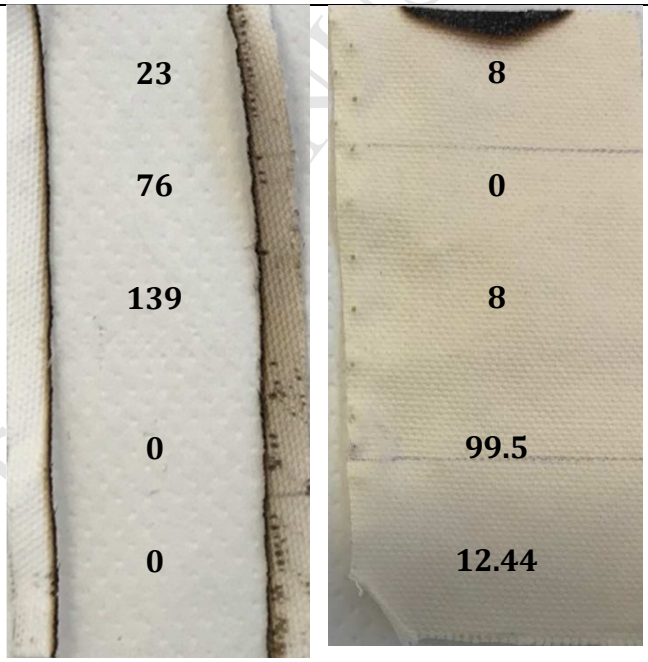

Vertical configuration			
	Flammability behaviour		
	Self-extinction	NO	YES

In order to understand the char composition and to investigate the mechanism of flame retardancy, achieved with the hybrid coating, after the vertical flame spread tests, SEM analysis and ATR-FTIR spectra of burned coated cotton fabrics were carried out. SEM micrographs (Figure 9) show that the charred region in the treated sample still maintains the shape of the original fibres and its weave structure, displaying only minor shrinkage. Fibres look very rough and show many bubbles on their surface: these findings are attributed to swelling and expansion of the coating due to its intumescent effect. It's possible to observe big bubbles on the surfaces of charred layer of FR cotton sample. These bubble char not only inhibits the release of flammable gases from cellulose degradation but also prevents the heat source to convey heat to the cellulosic substrate ~~and insulates the oxygen source~~ [52]. The intumescent layer protects the fibres from further burning, preserving the woven structure and fibre integrity, which is responsible for the self-extinguishing phenomenon of cotton. Besides, the results of the elemental analysis carried out on the same residue still indicate the presence of phosphorous and silicon, homogeneously distributed, notwithstanding the presence of carbon and oxygen, as for the control sample. This good performance was mainly produced by three components of developed molecule: first, the phosphorous group able to release P-based acids that catalyse the dehydration of cotton to form char. This char is able to prevent heat, fuel, and oxygen from being transferred from the flame to the fabric. Second, the deoxyribose units acted both as a

carbon source and blowing agents, with which a (poly)saccharide dehydrates to form char and releases water upon heating. Third, the nitrogen-containing base released ammonia, which can further induce char development and produce non-combustible gases such as N_2 and CO_2.

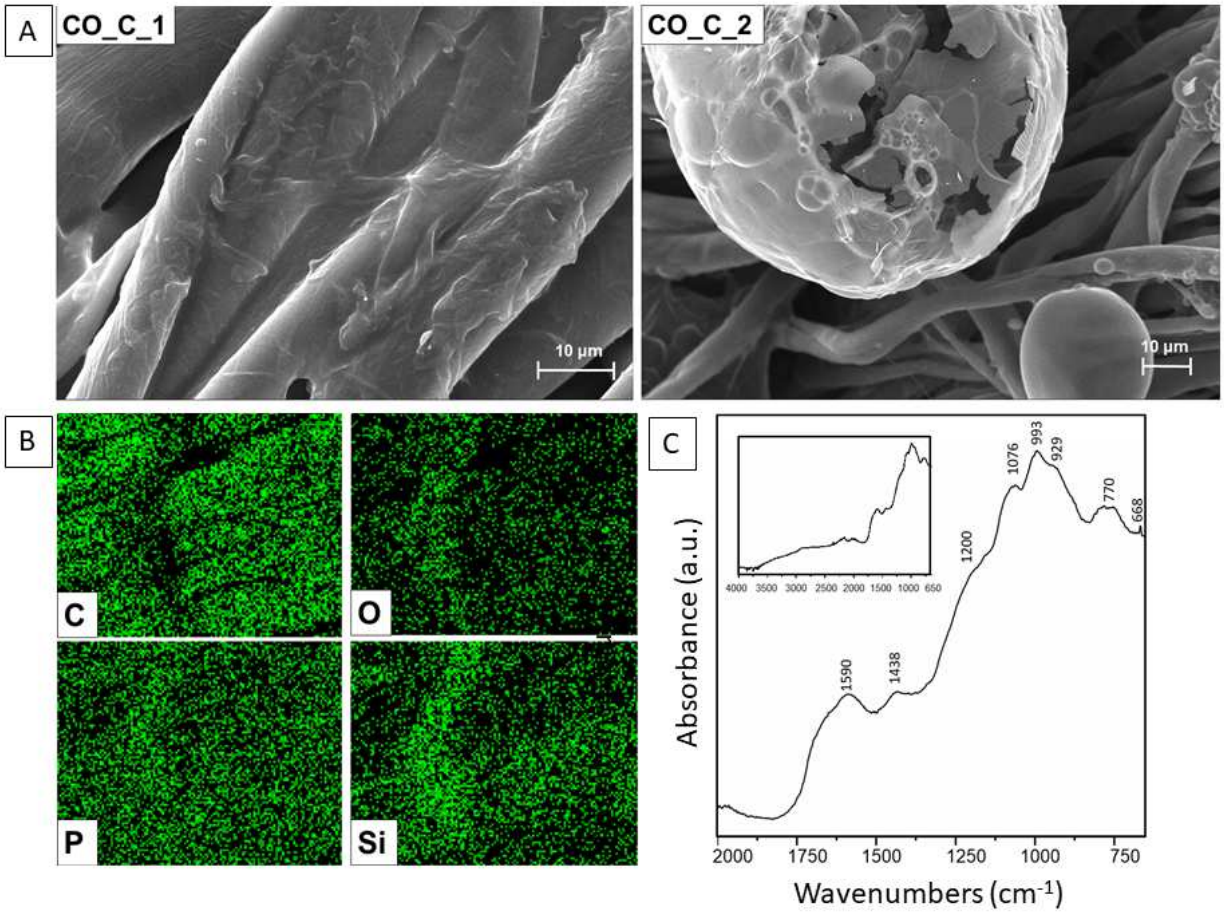

Fig. 9. A. SEM images of the residues of CO_T at different magnifications, coded as _1, _2, for x2.50 K, x1.00 K, respectively, **B.** EDX images of the treated sample; **C.** ATR-FT IR of treated cotton fabric pyrolyzed at 600°.

To investigate the chemical composition of the burned sol-gel coated fabric after the vertical flame spread test, the sample was examined by ATR-FTIR: its spectrum is shown in Figure 9C and detailed band assignments are provided alongside the spectrum. The presence of aromatic-type structure was confirmed by the intense band at around 1590 cm^{-1} and a shoulder at 1200 cm^{-1}, ascribed to the presence of polynuclear aromatic structures (-C=C- stretching) [53] and the vibration

of CH groups, out of plane bending, respectively. The shoulder peak at 1200 cm^{-1} may also comprise the signal assigned to the functionality of a phosphorus-nitrogen structure. Furthermore, the peaks in the region 1000–650 cm^{-1} may be assigned to the out of plane deformation vibrations of the ring [61]. Finally, the peaks at 1070 cm^{-1} are ascribable to the Si–O–Si stretching vibration that confirms the formation of a silica matrix in the char. These characteristic absorptions are in accordance with depolymerization of cellulose and formation of char [62]. From both analyses it is clear that the char of the treated sample seems to consist of phosphorous, carbon and silicon-rich compounds. The carbonaceous char that originates on the surface of the burning fabric during combustion is thus covered by silicates and phosphonates, hence creating an excellent physical barrier, which protects the substrate from heat and oxygen, and slowing down the escape of flammable volatiles generated during cellulose degradation.

4. Conclusions

A novel sol-gel based flame retardant containing phosphorus, nitrogen, and silicon was synthesized successfully, and its chemical structure was ~~fully~~ characterized by Fourier transform infrared spectrometry and nuclear magnetic resonance spectrometry (^{1}H NMR and $^{13}C/^{31}P$ NMR). After its application on cotton fabric, the combustion behaviour of the treated sample was investigated, confirming that the so obtained coating acts as an efficient flame retardant in the condensed phase. In particular, the presence of PGPTES lowers the decomposition temperature and favours the formation of char after pyrolysis; in addition, in forced combustion tests, the coating is responsible for the increase of TTI and the reduction of both HRR value and CO/CO_2 ratio for treated cotton sample. These results demonstrated the formation of a compact and thermostable char residue that effectively improved the thermal stability of cotton fabrics by hindering the formation of volatile species and favouring the creation of a stable char. It can be concluded that the hybrid GPTES-modified precursor can be potentially used as a new flame retardant replacing halogen-based

finishes in the field of flame retardant textile materials. Combining the above-mentioned advantages, it emerges as a promising candidate for the design of a next-generation of hybrid materials with breakthrough flame retardant performances. Further research will be developed in order to investigate the washing fastness of the proposed sol-gel coating and its influence on the mechanical properties of treated cotton fabrics.

References

[1] A.K. Yetisen, H. Qu, A. Manbachi, H. Butt, M.R. Dokmeci, J.P. Hinestroza, M. Skorobogatiy, A. Khademhosseini, S.H. Yun, Nanotechnology in Textiles, ACS Nano. 10 (2016) 3042–3068. doi:10.1021/acsnano.5b08176.

[2] A. Bhattacharyya, M. Joshi, Development of polyurethane based conducting nanocomposite fibers via twin screw extrusion, Fibers Polym. 12 (2011) 734–740. doi:10.1007/s12221-011-0734-8.

[3] M. Joshi, A. Bhattacharyya, Nanotechnology – a new route to high-performance functional textiles, Text. Prog. 43 (2011) 155–233. doi:10.1080/00405167.2011.570027.

[4] J. Alongi, J. Tata, F. Carosio, G. Rosace, A. Frache, G. Camino, A Comparative Analysis of Nanoparticle Adsorption as Fire-Protection Approach for Fabrics, Polymers (Basel). 7 (2014) 47–68. doi:10.3390/polym7010047.

[5] E. Busi, S. Maranghi, L. Corsi, R. Basosi, Environmental sustainability evaluation of innovative self-cleaning textiles, J. Clean. Prod. 133 (2016) 439–450. doi:10.1016/j.jclepro.2016.05.072.

[6] A.E. Danks, S.R. Hall, Z. Schnepp, The evolution of 'sol–gel' chemistry as a technique for materials synthesis, Mater. Horizons. 3 (2016) 91–112. doi:10.1039/C5MH00260E.

[7] H.-P. Boehm, The Chemistry of Silica. Solubility, Polymerization, Colloid and Surface Properties, and Biochemistry. VonR. K. Iler. John Wiley and Sons, Chichester 1979. XXIV, 886 S., geb. £ 39.50, Angew. Chemie. 92 (1980) 328–328. doi:10.1002/ange.19800920433.

[8] D.R. Brinker, C. J.; Clark, D. E.; Ulrich, BETIER CERAMICS THROUGH CHEMISTRY, Elsevier-North-Holland, New York, 1984.

[9] C.J. Brinker, Hydrolysis and condensation of silicates: Effects on structure, J. Non. Cryst. Solids. 100 (1988) 31–50. doi:10.1016/0022-3093(88)90005-1.

[10] B. Mahltig, H. Haufe, H. Böttcher, Functionalisation of textiles by inorganic sol–gel coatings, J. Mater. Chem. 15 (2005) 4385. doi:10.1039/b505177k.

[11] H. Schmidt, Considerations about the sol-gel process: From the classical sol-gel route to advanced chemical nanotechnologies, J. Sol-Gel Sci. Technol. 40 (2006) 115–130. doi:10.1007/s10971-006-9322-6.

[12] N.K. Sharma, C.S. Verma, V.M. Chariar, R. Prasad, Eco-friendly flame-retardant treatments for cellulosic green building materials, Indoor Built Environ. 24 (2015) 422–432. doi:10.1177/1420326X13516655.

[13] D.R. Baer, P.E. Burrows, A.A. El-Azab, Enhancing coating functionality using nanoscience and nanotechnology, Prog. Org. Coatings. 47 (2003) 342–356. doi:10.1016/S0300-9440(03)00127-9.

[14] R. Poli, C. Colleoni, A. Calvimontes, H. Polášková, V. Dutschk, G. Rosace, Innovative sol–gel route in neutral hydroalcoholic condition to obtain antibacterial cotton finishing by zinc precursor, J. Sol-Gel Sci. Technol. 74 (2015) 151–160. doi:10.1007/s10971-014-3589-9.

[15] H. Mahltig, B; Böttcher, Modified Silica Sol Coatings for Water-Repellent Textiles, J. Sol-Gel Sci. Technol. 27 (2003) 43–52.

[16] B. Mahltig, T. Textor, Combination of silica sol and dyes on textiles, J. Sol-Gel Sci. Technol. 39 (2006) 111–118. doi:10.1007/s10971-006-7744-9.

[17] F.-Y. Li, Y.-J. Xing, X. Ding, Immobilization of papain on cotton fabric by sol–gel method, Enzyme Microb. Technol. 40 (2007) 1692–1697. doi:10.1016/j.enzmictec.2006.09.007.

[18] A. Cireli, N. Onar, M.F. Ebeoglugil, I. Kayatekin, B. Kutlu, O. Culha, E. Celik, Development of flame retardancy properties of new halogen-free phosphorous doped SiO2 thin films on fabrics, J. Appl. Polym. Sci. 105 (2007) 3748–3756. doi:10.1002/app.26442.

[19] K.S. Huang, Y.H. Nien, K.C. Hsiao, Y.S. Chang, Application of DMEU/SiO2 gel solution in the antiwrinkle finishing of cotton fabrics, J. Appl. Polym. Sci. 102 (2006) 4136–4143. doi:10.1002/app.24246.

[20] C.-H. Xue, S.-T. Jia, H.-Z. Chen, M. Wang, Superhydrophobic cotton fabrics prepared by sol–gel coating of TiO 2 and surface hydrophobization, Sci. Technol. Adv. Mater. 9 (2008) 035001. doi:10.1088/1468-6996/9/3/035001.

635 [21] D. Štular, I. Jerman, I. Naglič, B. Simončič, B. Tomšič, Embedment of silver into temperature- and
636 pH-responsive microgel for the development of smart textiles with simultaneous moisture
637 management and controlled antimicrobial activities, Carbohydr. Polym. 159 (2017) 161–170.
638 doi:10.1016/j.carbpol.2016.12.030.
639 [22] S.H. Afzali, A.; Maghsoodlou, Modern application of nanotechnology in textile, in Nanostructured
640 Polymer Blends and Composites in Textiles, Apple Academic Press and CRC Press, 2016.
641 [23] B. Vasiljevic, J.; Hadzic, S.; Jerman, I.; Cerne, L.; Tomsic, B.; Medved, J.; Godec, M.; Orel, B.;
642 Simoncic, Study of flame-retardant finishing of cellulose fibers: organic-inorganic hybrid versus
643 conventional organophosphonate, Polym. Degrad. Stab. 98 (2013) 2602–2608. doi:j.
644 polymdegradstab.2013.09.020.
645 [24] J. Alongi, G. Malucelli, State of the art and perspectives on sol–gel derived hybrid architectures for
646 flame retardancy of textiles, J. Mater. Chem. 22 (2012) 21805–21809. doi:10.1039/C2JM32513F.
647 [25] T.-M. Nguyen, S. Chang, B. Condon, J. Smith, Fire Self-Extinguishing Cotton Fabric: Development
648 of Piperazine Derivatives Containing Phosphorous-Sulfur-Nitrogen and Their Flame Retardant and
649 Thermal Behaviors, Mater. Sci. Appl. 05 (2014) 789–802. doi:10.4236/msa.2014.511079.
650 [26] https://cottonaustralia.com.au/uploads/resources/CEK_Chap_9_Cotton_As_A_Consumer_Product.pdf.
651 [27] D. Wakelyn, P. J.; Bertoniere, N. R.; French, A. D.; Thibodeaux, Cotton Fiber Chemistry and
652 Technology, CRC Press (Taylor and Francis Group), 2007.
653 [28] Y. Jia, Y. Hu, D. Zheng, G. Zhang, F. Zhang, Y. Liang, Synthesis and evaluation of an efficient,
654 durable, and environmentally friendly flame retardant for cotton, Cellulose. 24 (2017) 1159–1170.
655 doi:10.1007/s10570-016-1163-z.
656 [29] R. Chénier, An Ecological Risk Assessment of Formaldehyde, Hum. Ecol. Risk Assess. An Int. J. 9
657 (2003) 483–509. doi:10.1080/713609919.
658 [30] M. Grumping, R.; Opel, M.; Petersen, Brominated dioxins and brominated flame retardants In irish
659 Cow‘S milk, Organohalogen Compd. 69 (2007) 912–915.
660 [31] Best Available Techniques (BAT) Reference Document for the Tanning of Hides and Skins, In:
661 Industrial Emissions Directive 2010/75/EU, (2013).
662 http://eippcb.jrc.ec.europa.eu/reference/BREF/TAN_Adopted552013.pdf.

[32] K. Kishore, K. Mohandas, Action of phosphorus compounds on fire-retardancy of cellulosic materials: A review, Fire Mater. 6 (1982) 54–58. doi:10.1002/fam.810060203.

[33] J.E. Hendrix, G.L. Drake, R.H. Barker, Pyrolysis and combustion of cellulose. III. Mechanistic basis for the synergism involving organic phosphates and nitrogenous bases, J. Appl. Polym. Sci. 16 (1972) 257–274. doi:10.1002/app.1972.070160201.

[34] M. Lewin, Synergism and catalysis in flame retardancy of polymers, Polym. Adv. Technol. 12 (2001) 215–222. doi:10.1002/pat.132.

[35] J. Alongi, C. Colleoni, G. Rosace, G. Malucelli, Phosphorus- and nitrogen-doped silica coatings for enhancing the flame retardancy of cotton: Synergisms or additive effects?, Polym. Degrad. Stab. 98 (2013) 579–589. doi:10.1016/j.polymdegradstab.2012.11.017.

[36] J. Alongi, C. Colleoni, G. Rosace, G. Malucelli, Thermal and fire stability of cotton fabrics coated with hybrid phosphorus-doped silica films, J. Therm. Anal. Calorim. 110 (2012) 1207–1216. doi:10.1007/s10973-011-2142-0.

[37] G. Brancatelli, C. Colleoni, M.R. Massafra, G. Rosace, Effect of hybrid phosphorus-doped silica thin films produced by sol-gel method on the thermal behavior of cotton fabrics, Polym. Degrad. Stab. 96 (2011) 483–490. doi:10.1016/j.polymdegradstab.2011.01.013.

[38] R.S. Kappes, T. Urbainczyk, U. Artz, T. Textor, J.S. Gutmann, Flame retardants based on amino silanes and phenylphosphonic acid, Polym. Degrad. Stab. 129 (2016) 168–179. doi:10.1016/j.polymdegradstab.2016.04.012.

[39] E. Guido, J. Alongi, C. Colleoni, A. Di Blasio, F. Carosio, M. Verelst, G. Malucelli, G. Rosace, Thermal stability and flame retardancy of polyester fabrics sol–gel treated in the presence of boehmite nanoparticles, Polym. Degrad. Stab. 98 (2013) 1609–1616. doi:10.1016/j.polymdegradstab.2013.06.021.

[40] S. Hribernik, M.S. Smole, K.S. Kleinschek, M. Bele, J. Jamnik, M. Gaberscek, Flame retardant activity of SiO2-coated regenerated cellulose fibres, Polym. Degrad. Stab. 92 (2007) 1957–1965. doi:10.1016/j.polymdegradstab.2007.08.010.

[41] X. Guillory, A. Tessier, G.-O. Gratien, P. Weiss, S. Colliec-Jouault, D. Dubreuil, J. Lebreton, J. Le Bideau, Glycidyl alkoxysilane reactivities towards simple nucleophiles in organic media for

improved molecular structure definition in hybrid materials, RSC Adv. 6 (2016) 74087–74099. doi:10.1039/C6RA01658H.

[42] L. Gabrielli, L. Connell, L. Russo, J. Jiménez-Barbero, F. Nicotra, L. Cipolla, J.R. Jones, Exploring GPTMS reactivity against simple nucleophiles: chemistry beyond hybrid materials fabrication, RSC Adv. 4 (2014) 1841–1848. doi:10.1039/C3RA44748K.

[43] G. Rosace, E. Guido, C. Colleoni, M. Brucale, E. Piperopoulos, C. Milone, M.R. Plutino, Halochromic resorufin-GPTMS hybrid sol-gel: Chemical-physical properties and use as pH sensor fabric coating, Sensors Actuators B Chem. 241 (2017) 85–95. doi:10.1016/j.snb.2016.10.038.

[44] L.S. Connell, L. Gabrielli, O. Mahony, L. Russo, L. Cipolla, J.R. Jones, Functionalizing natural polymers with alkoxysilane coupling agents: reacting 3-glycidoxypropyl trimethoxysilane with poly(γ-glutamic acid) and gelatin, Polym. Chem. 8 (2017) 1095–1103. doi:10.1039/C6PY01425A.

[45] M.R. Plutino, E. Guido, C. Colleoni, G. Rosace, Effect of GPTMS functionalization on the improvement of the pH-sensitive methyl red photostability, Sensors Actuators B Chem. 238 (2017) 281–291. doi:10.1016/j.snb.2016.07.050.

[46] E. Guido, C. Colleoni, K. De Clerck, M.R. Plutino, G. Rosace, Influence of catalyst in the synthesis of a cellulose-based sensor: Kinetic study of 3-glycidoxypropyltrimethoxysilane epoxy ring opening by Lewis acid, Sensors Actuators B Chem. 203 (2014) 213–222. doi:10.1016/j.snb.2014.06.126.

[47] J. Vasiljević, I. Jerman, G. Jakša, J. Alongi, G. Malucelli, M. Zorko, B. Tomšič, B. Simončič, Functionalization of cellulose fibres with DOPO-polysilsesquioxane flame retardant nanocoating, Cellulose. 22 (2015) 1893–1910. doi:10.1007/s10570-015-0599-x.

[48] G. Socrates, Infrared and Raman Characteristic Group Frequencies: Tables and Charts, 3rd editio, Wiley-Blackwell, 2004.

[49] C. Schramm, W.H. Binder, R. Tessadri, Durable Press Finishing of Cotton Fabric with 1,2,3,4-Butanetetracarboxylic Acid and TEOS/GPTMS, J. Sol-Gel Sci. Technol. 29 (2004) 155–165. doi:10.1023/B:JSST.0000023850.97771.7d.

[50] F. Branda, G. Malucelli, M. Durante, A. Piccolo, P. Mazzei, A. Costantini, B. Silvestri, M. Pennetta, A. Bifulco, Silica Treatments: A Fire Retardant Strategy for Hemp Fabric/Epoxy Composites, Polymers (Basel). 8 (2016) 313. doi:10.3390/polym8080313.

[51] C. Colleoni, I. Donelli, G. Freddi, E. Guido, V. Migani, G. Rosace, A novel sol-gel multi-layer approach for cotton fabric finishing by tetraethoxysilane precursor, Surf. Coatings Technol. 235 (2013) 192–203. doi:10.1016/j.surfcoat.2013.07.033.

[52] G. Rosace, A. Castellano, V. Trovato, G. Iacono, G. Malucelli, Thermal and flame retardant behaviour of cotton fabrics treated with a novel nitrogen-containing carboxyl-functionalized organophosphorus system, Carbohydr. Polym. 196 (2018) 348–358. doi:10.1016/j.carbpol.2018.05.012.

[53] C.-H. Chiang, H. Ishida, J.L. Koenig, The structure of γ-aminopropyltriethoxysilane on glass surfaces, J. Colloid Interface Sci. 74 (1980) 396–404. doi:10.1016/0021-9797(80)90209-X.

[54] J.-D. Zuo, S.-M. Liu, Q. Sheng, Synthesis and Application in Polypropylene of a Novel of Phosphorus-Containing Intumescent Flame Retardant, Molecules. 15 (2010) 7593–7602. doi:10.3390/molecules15117593.

[55] A.M. Grancaric, C. Colleoni, E. Guido, L. Botteri, G. Rosace, Thermal behaviour and flame retardancy of monoethanolamine-doped sol-gel coatings of cotton fabric, Prog. Org. Coatings. 103 (2017) 174–181. doi:10.1016/j.porgcoat.2016.10.035.

[56] J. Alongi, G. Malucelli, Cotton flame retardancy: state of the art and future perspectives, RSC Adv. 5 (2015) 24239–24263. doi:10.1039/C5RA01176K.

[57] J.D. Jovanovic, M.N. Govedarica, P.R. Dvornic, I.G. Popovic, The thermogravimetric analysis of some polysiloxanes, Polym. Degrad. Stab. 61 (1998) 87–93. doi:10.1016/S0141-3910(97)00135-3.

[58] J. Alongi, A. Frache, G. Malucelli, G. Camino, Multi-component flame resistant coating techniques for textiles, in: Handb. Fire Resist. Text., Elsevier, 2013: pp. 68–93. doi:10.1533/9780857098931.1.68.

[59] T.-L. Xing, J. Liu, S.-W. Li, G.-Q. Chen, Thermal properties of flame retardant cotton fabric grafted by dimethyl methacryloyloxyethyl phosphate, Therm. Sci. 16 (2012) 1472–1475. doi:10.2298/TSCI1205472X.

[60] M. Sevilla, A.B. Fuertes, The production of carbon materials by hydrothermal carbonization of cellulose, Carbon N. Y. 47 (2009) 2281–2289. doi:10.1016/j.carbon.2009.04.026.

[61] M. Nguyen, M. Al-Abdul-Wahid, K. Fontenot, E. Graves, S. Chang, B. Condon, C. Grimm, G.

Lorigan, Understanding the Mechanism of Action of Triazine-Phosphonate Derivatives as Flame Retardants for Cotton Fabric, Molecules. 20 (2015) 11236–11256. doi:10.3390/molecules200611236.

[62] S. Soares, G. Camino, S. Levchik, Comparative study of the thermal decomposition of pure cellulose and pulp paper, Polym. Degrad. Stab. 49 (1995) 275–283. doi:10.1016/0141-3910(95)87009-1.

HIGHLIGHTS

- NMR analysis confirms the functionalization of GPTES sol-gel precursor with PMIDA.
- PMIDA acts as nitrogen and phosphorous source in the P/N flame retardant synergism.
- The concurrent presence of Si, P and N enhances cellulose dehydration mechanism.
- The final residue for treated cotton sample, after cone calorimetry test, is 26%.
- Self-extinguishing properties are achieved by the treated cellulose-based fabric.